Biochemical Definition of `harsh' Vs. `mild' Detergents For Membrane Protein Solubilization

ARTICLE *in* BIOPHYSICAL JOURNAL · JANUARY 2010

Impact Factor: 3.97 · DOI: 10.1016/j.bpj.2009.12.290

3 AUTHORS, INCLUDING:

Arianna Rath

SickKids

32 PUBLICATIONS **768** CITATIONS

SEE PROFILE

BIOCHEMISTRY
including biophysical chemistry & molecular biology

Article

pubs.acs.org/biochemistry

Sequence Hydropathy Dominates Membrane Protein Response to Detergent Solubilization

Vincent G. Nadeau,[†,‡] Arianna Rath,[†] and Charles M. Deber*[,†,‡]

[†]Division of Molecular Structure & Function, Research Institute, Hospital for Sick Children, Toronto, Ontario, Canada M5G 1X8
[‡]Department of Biochemistry, University of Toronto, Toronto, Ontario, Canada M5S 1A8

ABSTRACT: The ability to predict from amino acid sequence how membrane protein structures will respond to detergent solubilization would significantly facilitate experimental characterization of these molecules. Here we have investigated and compared the response to solubilization by the "mild" *n*-dodecyl-*β*-D-maltoside (DDM) and "harsh" sodium dodecyl sulfate (SDS) of wild-type and point mutant "hairpin" (helix−loop−helix) membrane proteins derived from the third and fourth TM segments of the human cystic fibrosis transmembrane conductance regulator (CFTR) and the intervening extracellular loop. Circular dichroism spectroscopy, size-exclusion chromatography, and pyrene fluorescence spectroscopy were used to evaluate the secondary structures, hairpin−detergent complex excluded volumes, and hairpin compactness of the detergent-solubilized sequences. Sequence hydrophobicity is found to be the dominant factor dictating membrane protein response to detergent solubilization by DDM and SDS, with hairpin secondary structure exquisitely sensitive to mutation when DDM is used for solubilization. DDM and SDS differ principally in their ability to promote approach of TM segment ends, although hairpin compactness remains sensitive to point mutations. Our overall findings suggest that protein−protein and protein−detergent interactions are determined concomitantly, with the net hydropathy of residues exposed to detergent dominating the observed properties of the solubilized protein.

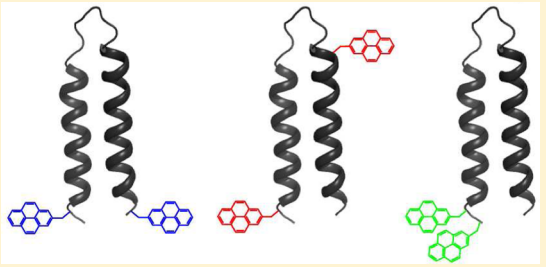

Proteins embedded in the membrane represent ∼20−30% of the human genome[1] and act as the transporters, sensors, and gates that connect the cell to its surroundings. These molecules are characterized by the presence of transmembrane (TM) regions—bilayer-embedded polypeptide sequences that are enriched in hydrophobic residues—and are categorized into two structural groups based on TM domain secondary structure. The TM sequences of helical bundle membrane proteins typically span the bilayer in *α*-helical conformation and are found in cytoplasmic membranes, while the TM regions of an important class of *β*-barrel membrane proteins traverse the outer membranes of bacteria and mitochondria as *β*-sheets. The high hydrophobicity of their TM domains causes membrane proteins to aggregate in water in the absence of the membrane bilayer; however, membrane protein structural biology and a large proportion of other biophysical and biochemical investigations require that the protein of interest is maintained in a membrane-free environment. Agents that render membrane proteins water-soluble in the absence of membranes are thus indispensable in membrane protein research.

Amphipathic compounds classified as surfactants by physical chemists but commonly referred to as detergents by biologists [see refs 2−4] are the most widely used membrane protein solubilizers [reviewed in ref 5]. These molecules are composed of at least one polar group (or "head") and one apolar group (or "tail"), typically an alkyl chain, and are available in various combinations of headgroup charge (anionic, cationic, zwitterionic, or neutral), tail group length, and tail group chemistry (hydrocarbon, fluorocarbon, etc.). Detergents prevent membrane protein aggregation in water by adsorbing to TM regions, sequestering these hydrophobic surfaces away from water and generally away from one another; at sufficiently high detergent concentrations [typically above the critical micelle concentration (cmc)[5]], the resulting protein−detergent complexes are water-soluble. Under ideal solubilization conditions, the structural integrity of the membrane protein is preserved within the protein−detergent complex. This may be achieved when a detergent adsorbs only to the formerly lipid-exposed membrane protein surfaces and leaves both extramembranous regions and sites of protein−protein contacts untouched,[6] such that the bilayer is replaced with a continuous belt of detergent molecules [see ref 3].

Interactions of proteins with detergents, and the structures of protein−detergent complexes, depend upon many factors: polypeptide sequence, secondary structure propensity, protein:detergent ratio, detergent type (e.g., headgroup charge, length of acyl chain), detergent concentration, the stability and shape of micellar structures, and solvent conditions such as pH, ionic strength, and temperature [reviewed in refs 2, 4, and 7]. It is perhaps not surprising, then, that determination of the detergent and buffer conditions needed to maintain the structural integrity of a solubilized membrane protein is an empirical and frequently time-consuming process.[8] The search

Received: December 14, 2011
Revised: June 7, 2012
Published: July 10, 2012

for appropriate solubilization conditions may be guided, in part, by categorization of detergents according to their propensity to preserve or disrupt membrane protein structure (classically termed "mild" and "harsh", respectively), with longer tail length, larger headgroup size, and neutral headgroup charge having been identified as properties compatible with structure preservation [see ref 5]. However, the responses of membrane protein structures to detergent solubilization trend only generally with detergent physicochemical properties. For example, *n*-dodecyl-*β*-D-maltoside (DDM), a prototypical "mild" hydrocarbon detergent with a 12-carbon (C12) tail and a neutral carbohydrate headgroup, facilitates the crystallization of "challenging" membrane proteins,[5] whereas pairing an anionic sulfate headgroup with the same C12 hydrocarbon tail, as in the prototypical "harsh" detergent sodium dodecyl sulfate (SDS), results in a molecule that denatures certain membrane proteins[9−15] yet preserves interactions between TM domains in several instances [e.g., refs 16−20].

The ability to predict from amino acid sequence how membrane protein structure will respond to solubilization by a given detergent would significantly facilitate experimental characterization of these proteins. As a step toward achieving this goal, in this work we have investigated the response of wild-type (WT) and point mutant "hairpin" membrane proteins—derived from the third and fourth TM segments of the human cystic fibrosis transmembrane conductance regulator (CFTR) and the intervening cellular loop (TM3/4)—to solubilization by DDM and by SDS. Circular dichroism (CD) spectroscopy, size-exclusion chromatography (SEC), and pyrene fluorescence spectroscopy are used to evaluate the secondary structures, hairpin−detergent complex excluded volumes, and relative hairpin compactness of the DDM-solubilized or SDS-solubilized sequences. Sequence hydrophobicity is found to be the dominant factor dictating membrane protein−detergent interactions, with hairpin secondary structure exquisitely sensitive to mutation when DDM is used for solubilization.

EXPERIMENTAL PROCEDURES

Assignment of Hairpin Residues to TM3, TM4, and Loop Regions. TM regions were predicted from the sequence of full-length CFTR (NCBI Reference Sequence: NP_000483.3) using the default settings of 11 unique TM helix identification algorithms [SOSUI,[21] PHDhtm,[22] SPLIT,[23] HMMTOP,[24] TM Finder,[25] OCTOPUS,[26] MEMSAT3,[27] DAS,[28] SCAMPI,[29] and PRO/PRODIV[30]]; the latter two programs were each run in two modes, resulting in a total of 13 predictions of membrane-embedded residues. CFTR residues assigned as membrane-embedded in at least 9/13 of these predictions were considered as helical TM sequences.

CFTR Helical Hairpin Proteins. Human CFTRTM3/4 hairpins were expressed from a previously described pET32a plasmid encoding a thioredoxin fusion to residues 194−241 of CFTR,[31,32] with a Cys-to-Ala replacement at residue 225 to facilitate purification[33] and to prevent conjugation to Cys-reactive species. Hairpins produced from this construct have N-terminal and C-terminal extensions that encode an S-tag epitope for Western blot detection and a hexahistidine sequence (GSGMKETAAAKFERQHMDSPDLGTDDDDKAM and LEHHHHHH, respectively).

BL21(DE3) (EMD Biosciences) or BL21 Star (DE3) (Life Technologies) chemically competent cells were transformed with sequence-verified plasmids. A single freshly transformed colony was used to inoculate 10 mL of Luria−Bertani (LB) medium with 50 μg/mL ampicillin and culture grown at 37 °C with shaking at 250 rpm overnight. The culture was then diluted in 250 mL or 1 L of M9 minimal medium with 50 μg/mL ampicillin and grown under identical conditions to an OD600 of ∼0.6; when protein expression was induced with 0.1 mM IPTG, the culture was supplemented with an additional 50 μg/mL ampicillin and grown at room temperature overnight. Cells were harvested at 10000*g* for 20 min.

Pellets from 1 L of culture were lysed by sonication in purification buffer [0.1% (w/v) Triton, 20 mM Tris-HCl (pH 8.0), 150 mM NaCl, 10 mM *β*-mercaptoethanol, and 5 mM imidazole]. Cellular debris was removed by centrifugation at 27000*g* for 20 min and supernatant mixed with 4−5 mL of 1:1 Ni-NTA agarose resin:purification buffer slurry (Qiagen) and gently rocked overnight at room temperature. Resin was washed three times with 50 mL of purification buffer with 5, 10, and 20 mM imidazole and bound protein eluted with 4 × 10 mL purification buffer with 405 mM imidazole. The thioredoxin fusion was removed from eluate by supplementation with 10−25 units thrombin (EMD) and gentle rocking at room temperature overnight.

Cleaved protein was purified by reverse-phase high performance liquid chromatography (RP-HPLC) on a 250 mm × 9.60 mm 10 μ 300 Å Chromegabond TMS C1 column (ES Industries) or a 250 mm × 10.0 mm Jupiter 5 μ 300 Å C4 column (Phenomenex) with a Waters 600 pump. Gradients utilized were linear 5−95% aqueous acetonitrile or linear 5−95% aqueous isopropanol (Caledon Laboratory Chemicals, Caledon, ON) in 0.1% TFA (PSIG Polycentric Services Inc., Saint-Laurent, QC). Protein peaks were collected, mass and purity were evaluated by matrix-assisted laser desorption ionization and/or electrospray ionization mass spectrometry (MALDI- and/or ESI-MS), and each purified sample (≥95%) was frozen on dry ice and lyophilized to powder.

Size-Exclusion Chromatography (SEC). SEC was performed on a 300 × 7.80 mm BioSep-SEC-S2000 column (Phenomenex) in a mobile phase of 50 mM NaPi, pH 7, 0.05% (w/v) DDM. This concentration of DDM (∼1 mM) exceeds by ∼5× the CMC of this detergent, measured as 0.15−0.33 mM in water[34−36] and 0.21 mM in 20 mM acetate buffer, pH 4.9.[37] The column was equilibrated with 5−10 column volumes of mobile phase, and a flow rate of 0.5 mL/min delivered by a Waters 600 pump was used for all experiments. Purified hairpins (0.025 mg) were dissolved in 500 μL of mobile phase buffer and equilibrated at room temperature overnight. Each sample was bath-sonicated for 10 min from one to three times and then centrifuged for 15 min at maximum speed in a microcentrifuge prior to injection of 300 μL of each hairpin solution. The remainder of each sample was reserved for circular dichroism spectroscopy (see below). Elution was detected by absorbance at 280 nm. Column void volume was estimated as the elution volume of 0.4 mg blue dextran (GE Healthcare).

Circular Dichroism (CD) Spectroscopy. Hairpin samples dissolved in mobile phase were diluted to a protein concentration of 10 μM. Three spectra were accumulated for each sample from 250 to 190 nm on a Jasco 720 CD spectrometer using a cuvette length 0.1 cm, a 4 s response time, a 2 nm bandwidth, and a 50 nm/min scan speed. Background spectra without protein were subtracted.

Pyrene Fluorescence Spectroscopy. WT and mutant hairpins used in pyrene excimer fluorescence studies incorpo-

rated two additional Cys residues, placed at the N- and C-terminal ends of the CFTR sequence encompassed by the hairpin [WT sequence GSGMKETAAAKFERQHMDSPDLGTDDDDDCKAMGLALAHFVWIAPLQVALLMGLIWELLQASAFAGLGFLIVLALFQAGLGLECHHHHHH]; Cys residues were introduced at positions four residues apart in the N-terminal extension of the WT sequence to serve as the excimer fluorescence positive control [hairpin sequence GSGMKETAAAKFERQHMDSPDLGTDCDDDCKAMGLALAHFVWIAPLQVALLMGLIWELLQASAFAGLGFLIVLALFQAGLGLEHHHHHH]; Cys residues were introduced at positions 32 residues apart in the WT background, at the N-terminal sides of the TM3 and TM4 sequences, to serve as the negative control for pyrene excimer emission [hairpin sequence GSGMKETAAAKFERQHMDSPDLGTDDDDDCKAMGLALAHFVWIAPLQVALLMGLIWELLQASCFAGLGFLIVLALFQAGLGLEHHHHHH]. Residue substitutions were made with the QuikChange site-directed mutagenesis kit (Stratagene) and verified by DNA sequencing.

To label hairpins, purified double-Cys hairpins were resuspended in 20−40 mL of labeling buffer [20 mM TrisHCl, pH 7.5, 0.5% (w/v) SDS, 1.5 mM tris(2-carboxyethyl)-phosphine (TCEP)] from lyophilized powder. A freshly prepared 1 mM solution of *N*-(1-pyrene)iodoacetamide (Life Technologies) in *N,N*-dimethylformamide (Caledon Laboratory Chemicals, Caledon, ON) was added dropwise to the resuspended hairpins. Reactions were blanketed with N_2 gas and incubated with shaking at room temperature in the dark for 16−72 h. After incubation, reaction mixtures were centrifuged to remove insoluble material prior to hairpin purification by RP-HPLC as described above. The proportion of purified hairpin molecules incorporating two pyrene moieties vs a single pyrene group (labeling ratio) was estimated from the mass spectrometric peak intensities of double-pyrene vs single-pyrene hairpins and found to be >70% in all cases.

Lyophilized labeled hairpins were resuspended in SEC mobile phase buffer (as above) or in 0.3% SDS, 50 mM Na phosphate, pH 7. The [SDS] employed exceeds 5 × cmc in this buffer.[31] Spectra were recorded postsolubilization in a 1 cm path length cuvette at an excitation wavelength of 345 nm with a 2 nm bandpass. Emission spectra were recorded three times from 370 to 550 nm in 1 nm increments with a 0.3 s integration time and a 4 or 6 nm bandpass and averaged. Background spectra without protein were subtracted. Spectra were initially obtained at total hairpin concentrations of 0.5, 1, 2, 5, 10, and 15 μM to evaluate any effects of molecular crowding on excimer peak intensity. Small levels of molecular crowding were observed with increasing concentrations evidenced by increases in excimer/monomer peak intensity in both doubly pyrene labeled hairpin constructs and free pyrene molecules (data not shown). Solutions of 2 μM were accordingly used for subsequent measurements to maximize emission intensity and minimize inner filter effects. Reference spectra of 4 μM free pyrene were recorded to confirm the absence of excimer peak at the effective pyrene concentration used with labeled proteins (data not shown). Monomer and excimer peak intensities were determined by integration of spectra from 370−440 nm and 441−550 nm, respectively. The excimer:monomer values (E:M) were calculated from the ratio of these intensities and normalized for any contribution of single-labeled hairpins to emission spectra by division with the appropriate labeling factor.

Quantitation of CFTR Helical Hairpin Proteins. Protein content of hairpins solubilized in 0.3% SDS or in 0.05% DDM buffer was assayed after sonication and/or incubation and centrifugation. The Micro BCA assay (Thermo Fisher) was used according to the manufacturer's directions. Samples were diluted 1/5 with ultrapure water before analysis to ensure that detergent amounts were noninterfering in the assay. Standard curves were prepared in appropriately diluted mobile phase buffer with manufacturer-supplied bovine serum albumin.

Statistical Analysis. Means ± SD were compared with unpaired two-tailed *t*-tests unless otherwise indicated. Linear fits and comparisons were performed with Prism Version 4.0a or OriginPro 8. *P* values of ≤0.01 were considered highly significant, >0.01 to ≤0.05 significant, and >0.05 to ≤0.1 of marginal significance.

RESULTS

Characteristics of the Hairpin Folding Model. The TM3/4 hairpins utilized in this work include residues 194−243, inclusive, of the wild-type human cystic fibrosis transmembrane conductance regulator, encompassing CFTR membrane-spanning sequences 3 and 4 and the intervening extracellular loop (ECL2).[38] Since the high-resolution structure of the membrane-embedded portion of CFTR is not yet available, residues were classified to TM helix or non-TM regions based on the output of prediction algorithms (see Experimental Procedures). TM regions of TM3/4 were then delimited based on assignment of a given residue as membrane-embedded in at least 9 of the 13 predictions. Based on this analysis, residues Ala^{198}-Trp^{216}, residues Ser^{222}-Leu^{240}, and residues Glu^{217}-Ala^{221} were assigned to the TM3, TM4, and the intervening loop region, respectively (Figure 1). The topology thus predicted for TM3/4—two α-helical TM domain sequences separated by a short loop—represents a useful membrane protein model system because it recapitulates the minimal model of helical membrane protein tertiary structure (Figure 1). The relatively modest size of the hairpin construct (87 residues) also permits the detection of sequence-dependent structural fluctuations that may be masked in larger membrane proteins. Further, the construct used generally displays expression levels sufficient for a variety of in-vitro characterization experiments in the presence of diverse single and multiple residue substitutions.[31,39−42] The mutants selected for study in the present work have a broad representation of mutant types and positions but also the required expression levels, along with a wide range of SDS binding levels, helicity levels (from CD), and detergent−protein particle size (from SEC).[31] The ES/SE mutant was included as an "isohydropathic" control.

Secondary Structure of Hairpins Solubilized in DDM and SDS. Circular dichroism (CD) spectroscopy was used to evaluate the secondary structure content of hairpins after DDM solubilization. Dual absorption minima at 208 and 222 nm were observed in the spectrum of the WT and of each mutant (Figure 2A, left), consistent with formation of α-helical secondary structure by the proteins. However, the intensities of these minima were not consistent. The intensity of mean residue ellipticity at 222 nm, for example, ranged by ∼20 000 deg cm^2 dmol^{-1} among the hairpin sequences (compare E217V and V232D, Figure 2A, left), a result that might not initially be anticipated for a "mild" detergent. In fact, our group has previously observed that variable levels of secondary structure are a hallmark of hairpin dissolution in the "harsh" detergent SDS.[31] Upon comparison and statistical analysis of the hairpin

dx.doi.org/10.1021/bi201853n | *Biochemistry* 2012, 51, 6228−6237

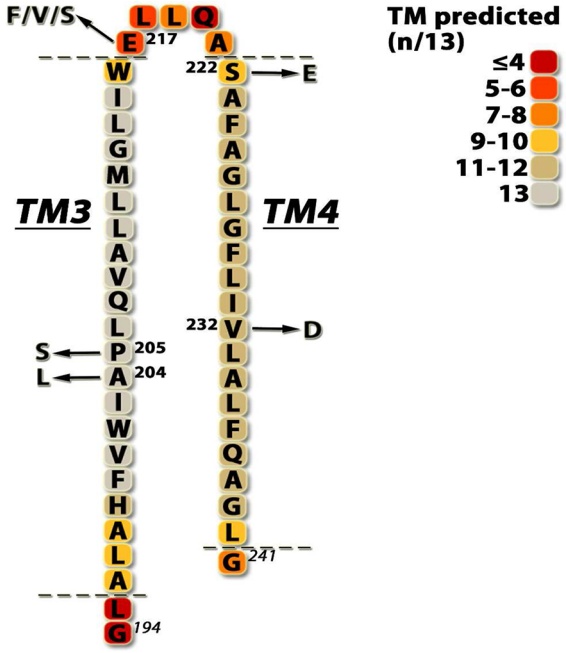

Figure 1. TM3/4 hairpin constructs. The CFTR TM3/4 sequence is shown in black text. Shading indicates the number of times (n) that each residue was identified as membrane-embedded in 13 outputs from a variety of TM α-helix prediction programs (see Experimental Procedures). Residues predicted as membrane-embedded in at least 9/13 outputs were considered as TM-located, as indicated by the positions of dashed lines. Ends of the human CFTR sequence in the TM3/4 construct are labeled with residue numbering in italics. The positions and identities of residue substitutions studied in this work are indicated by arrows and residue numbering in bold.

CD spectra in DDM and SDS (Figure 2A, left and right panels), we found that the overall intensities of spectra obtained for the DDM-solubilized hairpins differed from those obtained in SDS principally in that the former detergent supported a greater content of helical secondary structure; thus, the group-averaged mean residue ellipticity value at 222 nm among DDM-solubilized hairpins was significantly different from the group average after dissolution by SDS (-27500 ± 6800 deg cm^2 dmol^{-1} vs -21000 ± 4700 deg cm^2 dmol^{-1}, respectively, $p = 3.3 \times 10^{-5}$). We further noted that the spectra of mutant hairpins solubilized in DDM exhibited a gradation of intensities, whereas SDS-solubilized mutant spectra could be divided into "low helicity" (WT, V232D, A204L, and P205S) or "high helicity" (E217V, ES/SE, and E217F) clusters. Interestingly, these two groupings corresponded to the location of their residue substitutions in the TM or loop regions of the hairpin sequence, respectively (Figure 1). Comparison of mean residue ellipticity values at 222 nm confirmed that the "low helicity" and "high helicity" groups of hairpin mutants were statistically distinguishable in helix content after SDS solubilization ($p = 0.0013$ between groups in SDS, by ANOVA) but that this distinction between groups disappeared in DDM ($p = 0.306$ between groups in DDM, by ANOVA). On an individual sequence level, the intensity of the helix signal at 222 nm of the WT hairpin in DDM exceeded that observed in SDS (-21800 ± 3000 vs -17800 ± 2100 deg cm^2 dmol^{-1}, respectively, $p = 0.025$).

The mutant-dependent changes in helicity observed in DDM were then normalized to the secondary structure content of the WT hairpin and plotted as a function of amino acid sequence hydropathy changes (Figure 2B, left); a strong and significant direct correlation of helicity and hairpin hydrophobicity in DDM was observed ($R^2 = 0.75$, $p = 0.026$, Figure 2B, left). This relationship was statistically indistinguishable from that previously observed among this group of hairpins in SDS [($R^2 = 0.71$, $p = 0.036$, Figure 2B, right; see also ref 31] ($p = 0.385$ for slopes of best-fit lines). The helical secondary structure of hairpins solubilized in DDM thus exhibits a dependence on sequence hydropathy changes equal in magnitude to those solubilized in SDS. The correlation of hydropathy levels in TM3/4 mutants and helicity in both detergents was also apparent in the rank ordering of mutants according to their molar residue ellipticity at 222 nm (Figure 2, right), with the exception of three mutants: E217F, E217V, and ES/SE (Figure 2A). The former two are very hydrophobic mutations that remain the most helical constructs in each detergent, albeit with opposite order. Interestingly, we noted the large rank order change of ES/SE; this mutant largely differs from the others studied in that it does not change the bulk hydrophobicity of the hairpin.

Size/Shape of Hairpin–DDM and Hairpin–SDS Complexes. The ability of DDM to generally support more helical secondary structure than SDS could thus not be traced to any inherent difference in the dependence of hairpin secondary structure on hydrophobicity changes. We therefore hypothesized that a difference in the structures of the hairpin–detergent complexes formed by DDM might be involved. The relative sizes and/or shapes of hairpin–DDM complexes were accordingly assessed by size-exclusion chromatography (SEC). This technique separates particles as a function of hydrodynamic volume and thus reports a combination of the particle size and shape of protein–detergent complexes. Shorter SEC elution volumes generally indicate larger sized protein–detergent complexes, and vice versa [reviewed in ref 43], although those with elongated rather than compact and/or spherical shapes may exhibit anomalous elution profiles.[44] The elution volumes of hairpins solubilized in DDM and applied individually to a pre-equilibrated size-exclusion column were accordingly not utilized as an absolute measure of hairpin–detergent complex stoichiometry and/or protein mass. Rather, they were ranked and compared among mutants.

We observed that each hairpin–DDM complex eluted as a single peak (typical elution profiles shown in Figure 3A), with the exception of the ES/SE–DDM species, where a minor peak with a larger elution volume was observed (data not shown); the elution volume of the major peak was used for further analysis. The WT and mutant sequences complexed with DDM exhibited variable elution volumes, with ES/SE and V232D eluting earliest and latest from the column, respectively (Figure 3B, left). Inspection of the rank ordering of the elution times of the WT and mutant hairpin–DDM complexes indicated a generally parallel trend with helix content and with sequence hydrophobicity changes such that hairpins with larger protein–DDM complex shape/size tended to exhibit greater helical secondary structure content and enhanced hydrophobicity. The ES/SE mutant, however, is an exception to this general trend. The ES/SE–DDM complex has the shortest SEC elution time, suggesting it maintains the largest effective protein–DDM complex size, yet is ranked third lowest in helix content (compare Figure 2A, left and Figure 3B).

The order of elution of WT and mutant hairpin–DDM complexes was generally similar to that previously observed[31] among hairpin–SDS complexes (Figure 3B), since regression

dx.doi.org/10.1021/bi201853n | Biochemistry 2012, 51, 6228–6237

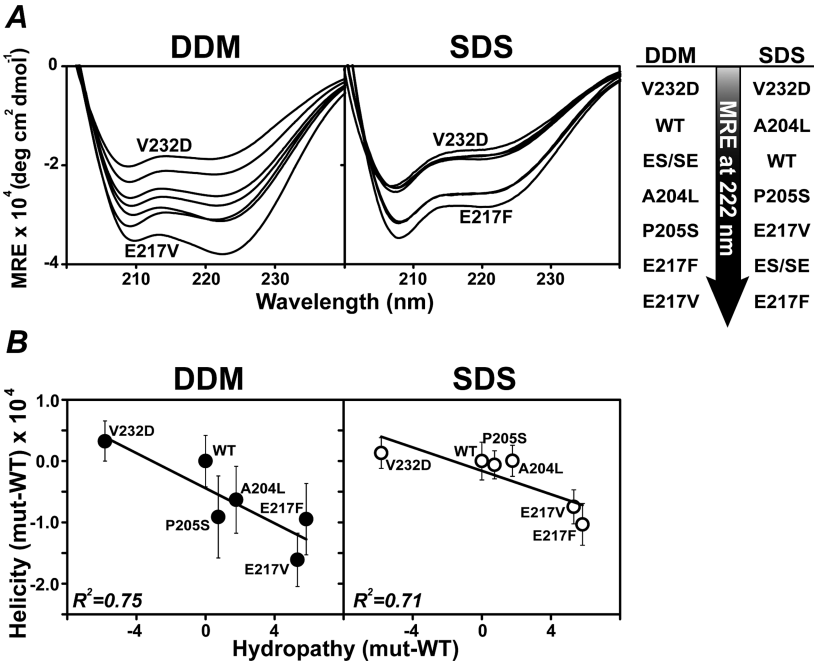

Figure 2. Circular dichroism spectra of TM3/4 mutants. (A) CD spectra of CFTR TM3/4 hairpins solubilized in DDM (left) and SDS (right). The average of 4−6 independent measurements is shown. Mutants with largest and lowest levels of helicity at 222 nm are labeled. Rank ordering by helicity at 222 nm of hairpin−DDM complexes and hairpin−SDS complexes is given to the right of the spectra. SDS data adapted from.[31] (B) Correlation of TM3/4 sequence hydropathy with WT-normalized helicity values in DDM (left, slope = -1.4×10^3) and SDS (right, slope = -0.96×10^3). $N = 6$ for all plots, and lines of best fit are shown. Errors shown were propagated from average mean residue ellipticity values at 222 nm using standard formulas. Hydropathy values normalized to WT were averaged from six common scales such that positive hydropathy indicates increased apolarity and vice versa.[31] The isohydropathic ES/SE mutant was excluded from all plots.

analysis of the correlation among their elution volumes yields a slope of ∼1 ($R^2 = 0.88$, $p = 0.006$). However, we noted that the elution volumes of the V232D mutant (open circle, Figure 3B) placed this hairpin outside the 95% confidence interval of the line of best fit. TM3/4-V232D can therefore be considered to differ in its hydrodynamic properties following solubilization by DDM vs SDS. As a group, however, the hairpin−DDM complexes eluted earlier than the hairpin−SDS complexes ($p = 2.3 \times 10^{-29}$ by ANOVA); detergent-induced alterations in the gel matrix were excluded as the source of this difference, as column void volumes in DDM or SDS were statistically indistinguishable ($p = 0.77$; Figure 2B). Since reduced elution volumes generally indicate increased protein−detergent complex excluded volumes, the size/shape of the hairpin−DDM complexes was accordingly considered to be larger than that of hairpin−SDS complexes. Any combination of the larger headgroup excluded volume of DDM, its large micelle size,[5] a difference in micelle morphology, and/or increased stoichiometry of DDM binding to hairpins could thus underlie the reduced elution volumes of hairpin−DDM vs hairpin−SDS complexes.

Hairpin Compactness within DDM and SDS Complexes Studied by Pyrene Fluorescence. To examine more quantitatively the extent to which members of our hairpin library exist in folded conformations, we evaluated the compactness of DDM- or SDS-solubilized hairpins by exploiting the unique fluorescence properties of pyrene, a spatially sensitive probe of protein conformational changes.[32,45−48] The utility of pyrene as a structural probe arises from characteristic changes in its emission spectrum that report on its relative proximity to another pyrene molecule. Emission maxima in the 375−395 nm range are attributed to monomeric pyrene moieties, while the appearance of a broad, red-shifted emission maximum centered at ∼480 nm, concomitant with reduced monomer band intensity, indicates interaction of a ground state with an excited-state pyrene molecule to form an excited-state dimer or "excimer". Since excimer fluorescence is decreased and usually lost completely upon positioning of the interacting pyrene moieties >10 Å from one another,[49] we employ here an operational definition of "compactness" to indicate proximity of the TM3 and TM4 helices within this 10 Å distance. Hairpin constructs were accordingly covalently modified each with two pyrene groups, as shown schematically in Figure 4A (see Experimental Procedures for details of pyrene incorporation): in the WT hairpin and in each mutant sequence, pyrene moieties were conjugated at positions near the N-terminal end of TM3 and the C-terminal end of TM4 (Figure 4A, left). Two controls were also constructed in the WT sequence context: a positive control with pyrene moieties placed three residues apart (Figure 4A, right) and a negative control with pyrene moieties placed distal in the sequence (Figure 4A, center).

Pyrene fluorescence emission spectra of the WT hairpin, each mutant hairpin, and the positive and negative control sequences were obtained after solubilization in DDM or in SDS (Figure 4B) and helix−helix proximity was evaluated from each spectrum using the ratio of fluorescence emission intensity in the excimer and monomer regions (E:M ratio; see Experimental Methods for calculation details). Spectra collected from the positive control hairpin after solubilization in either detergent exhibited a high intensity, broad excimer emission band centered at ∼480 nm, confirming the requirement of optimized distance and packing angles of pyrene labels in this experiment. Thus, we expect the positive control excimer peak

dx.doi.org/10.1021/bi201853n | *Biochemistry* 2012, 51, 6228−6237

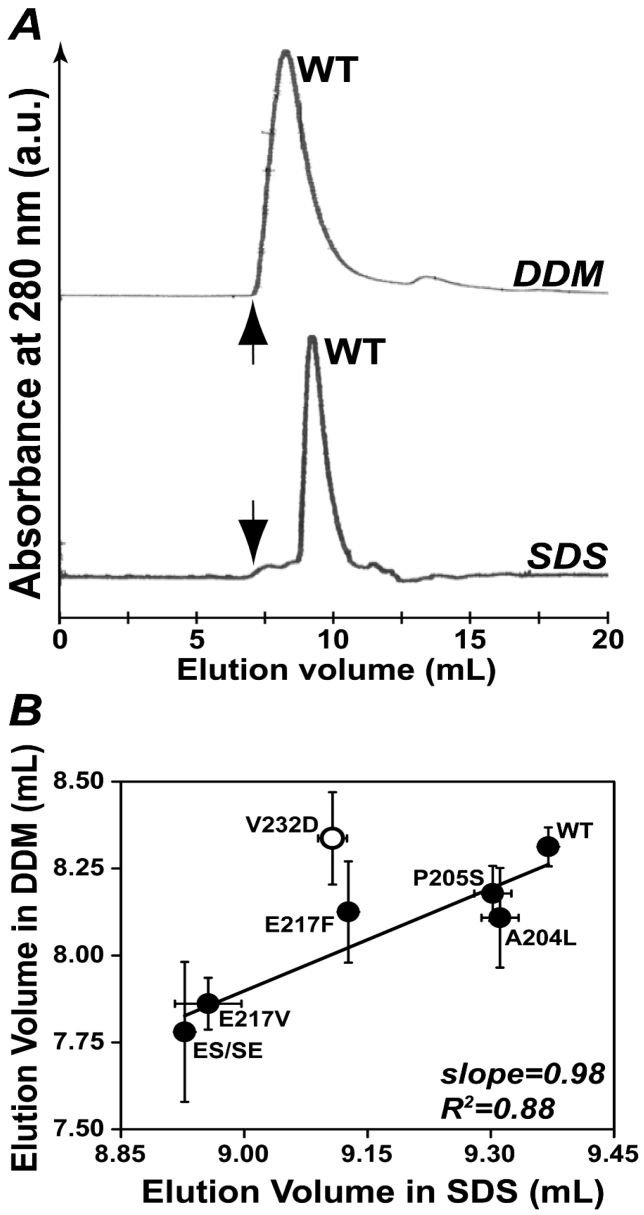

Figure 3. Size-exclusion chromatography of hairpin-detergent complexes. (A) Chromatogram of the WT hairpin−DDM complex (top) and WT hairpin−SDS complex (bottom). Arrows indicate column void volume after equilibration in micellar concentrations of DDM or SDS (see Experimental Procedures for details). (B) Correlation between SEC elution time in DDM and SDS for TM3/4 mutants. $N = 7$ for the plots; the line of best fit omits the outlier mutant V232D (open circle, data point outside the 95% confidence interval of the fit). Errors shown were propagated from average elution times using standard formulas. Note that the line of best fit has a near-unity slope, indicating that the relative order of elution is the same among the hairpin−DDM and hairpin−SDS complexes when V232D is excepted. SDS data adapted from ref 31.

(Figure 4B) to be representative of a much higher signal than any given mutant fully folded hairpin construct. This emission band was absent in the spectra of the negative control (Figure 4B, left and right).

In DDM (Figure 4B, left), we found that the P205S (E:M = 0.87 ± 0.20), E217V (E:M = 0.78 ± 0.06), E271F (E:M = 0.76 ± 0.12) and A204L spectra (E:M = 0.69 ± 0.02) each displayed excimer fluorescence, and the E:M ratio of each of these "compact" mutants was statistically distinct from the negative control in DDM (E:M = 0.52 ± 0.02, $4.7 \times 10^{-6} \leq p \leq 0.008$). The E:M ratios of the compact mutants were ~2-fold lower vs the positive control (E:M ratio 1.71 ± 0.16) as evidenced by statistically distinct E:M ratios ($2.6 \times 10^{-6} \leq p \leq 9.7 \times 10^{-4}$ vs positive control). In contrast, after SDS solubilization (Figure 4B, right), excimer emission above negative control (E:M = 0.21 ± 0.004) levels was present only in the A204L mutant (E:M = 0.32 ± 0.06, $p = 0.027$); the E217V mutant had an E:M ratio higher than the negative control, but this difference was of marginal significance (E:M = 0.28 ± 0.04, $p = 0.062$). Solubilization by the harsh detergent thus appeared largely incompatible with maintenance of a <10 Å distance between the pyrene molecules at the ends of TM3 and TM4.

DISCUSSION

Hairpin Secondary Structure in Mild and Harsh Detergents. Changes in helicity among the hairpin single point mutants are shown here to be equally dependent on sequence hydrophobicity in DDM and in SDS (Figure 2B), with ~70% of the variation in secondary structure attributable to global hydropathy changes. This result implies that a common property of the two detergents underlies the response of protein structure to DDM or SDS solubilization, likely hydrophobic interactions in each case between the C12 tail group and the protein sequence. This contention is supported by the direct correlation between hairpin helicity and SDS binding levels previously established[31] and observations that binding of DDM to polypeptides leads to helical secondary structure induction and depends upon sequence hydrophobicity.[37] The effects of the single point mutants on hairpin secondary structure in both detergents are thus dominated by mutant-modulated stabilization and/or alterations in the hairpin fold as manifested by gradations in the measured biophysical properties of the resulting protein−detergent complexes. This situation is rendered pictorially in Figure 5, where a hairpin TM4 mutant can variously retain its original fold or alter the nonmutated interface via rotation around the TM3, TM4, or both TM3 + TM4 major axes to create not only new helix−helix interfaces but concomitantly new faces of exposure to the detergent medium. This latter effect can then alter the mode—and extent—of detergent interactions with a given mutant hairpin. There is admittedly a "chicken-and-egg" aspect to this analysis, such that the interactions offered by a particular detergent to the protein can exert its influence as a determinant of the final population(s) of hairpin structure.

The largely equivalent response of helicity among point mutant hairpins to DDM and SDS solubilization seems at odds with the typical categorization of the former detergent as "mild" and the latter "harsh" to membrane protein structure. However, the higher baseline content of helical secondary structure adopted by the WT hairpin when solubilized in DDM vs SDS (Figure 2A) is consistent with the "mild" or at least "milder" classification of the former detergent. This helix stabilizing effect may originate from characteristics of the DDM−hairpin complex and/or from the detergent itself. Although not measured directly, our data are consistent with adsorption of a larger number of DDM monomers vs SDS monomers to the WT hairpin, resulting in a higher level of helix structure. The larger excluded volume observed on SEC of the WT−DDM vs WT−SDS complexes, a difference that is statistically significant ($p = 3.5 \times 10^{-8}$; Figure 3B), supports this notion.

dx.doi.org/10.1021/bi201853n | Biochemistry 2012, 51, 6228−6237

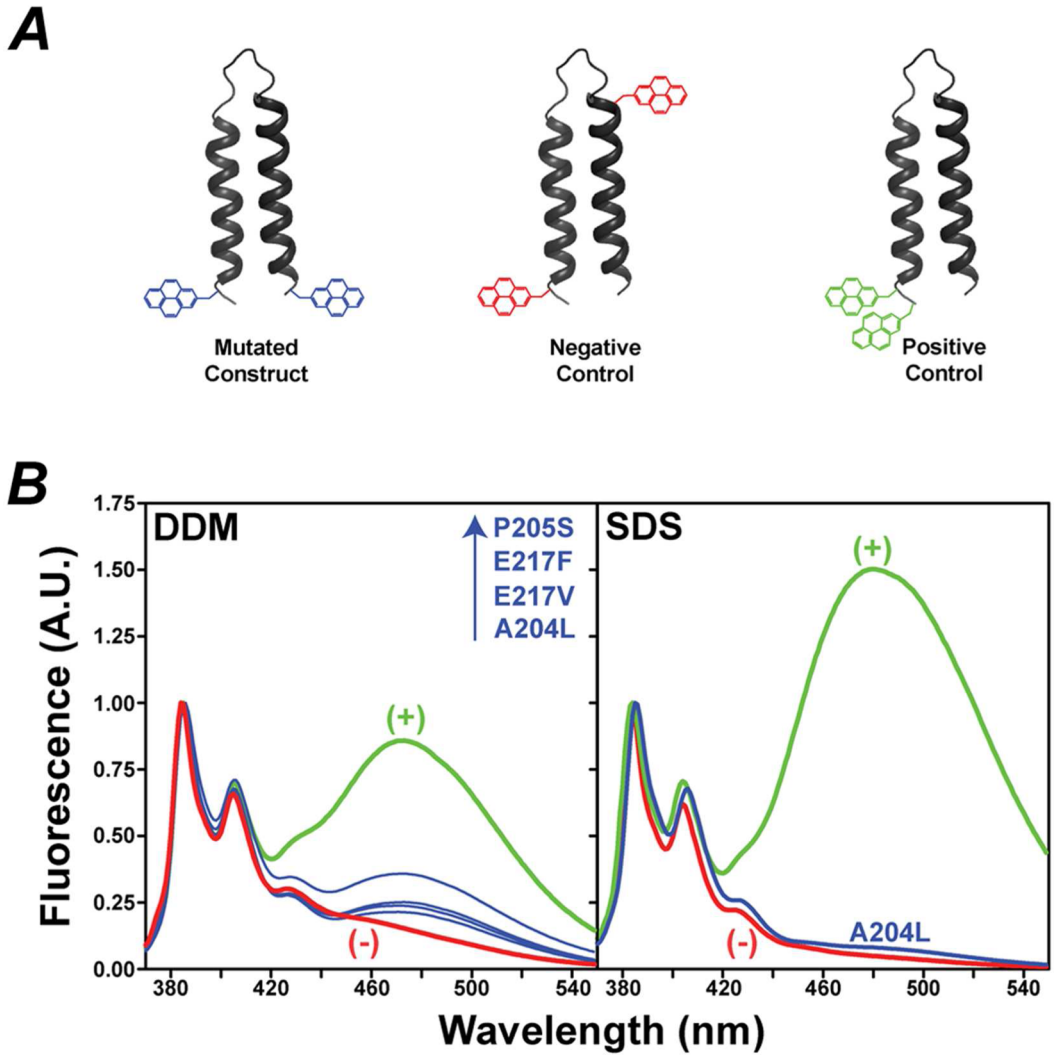

Figure 4. Pyrene fluorescence spectra of hairpin sequences. (A) Hairpin constructs used in pyrene excimer fluorescence studies, with the relative positions of the conjugated pyrene molecules shown schematically (see Experimental Procedures for sequences). TM sequences are indicated with helical secondary structure. (B) Pyrene fluorescence emission spectra of positive and negative control sequences [indicated as (+) and (−), respectively] and of the mutants solubilized in DDM (left) and in SDS (right) that exhibit an excimer:monomer ratio (E:M) above the negative control. Each spectrum represents the average of 3−9 independent experiments and was normalized to the intensity of the 385 nm monomer band. Spectra were not corrected for the contribution of single labeled species (see Experimental Procedures). Mutants not shown exhibited excimer fluorescence emission that did not exceed negative control values in DDM and/or SDS.

A further observation from the sets of CD curves shown in Figure 2 is that the spectra in SDS display ellipticity notably skewed toward the 208 nm lobe, while corresponding spectra in DDM generally have approximately equal ellipticity for the 208 and 222 nm lobes (exception: the loop-based E217V mutant). The skewing toward 208 nm may be a consequence of a higher content of "unstructured" regions in SDS relative to DDM, and hence CD spectra significantly overlap near 200 nm in the "mild" detergent. These latter observations are consistent with the notion that the anionic SDS may tend to fray helix ends—particularly for the Asp-rich TM3 N-terminus extension (see Experimental Procedures)—by lack of binding to this region, while the results in the neutral DDM medium likely arise more directly from levels of detergent binding generated by the sequence and construct conformation.

Hydropathy Dependence in Local Sequence Context: The Cases of ES/SE and V232D. The ES/SE−DDM and V232D mutants are distinguished among the groups of DDM- or SDS-solubilized hairpins in that each of these hairpin−detergent complexes exhibits an apparent excluded volume on SEC that is larger than expected based on their rankings in helicity and low E:M ratios (compare Figures 3B, 2B, and 4B). Because the excluded volume of protein−detergent complexes is not an absolute measure of binding stoichiometry or particle size when particles deviate from compact, spherical shapes, we can only conclude at present that the shapes and/or dynamics of the ES/SE−DDM complex and the V232D−SDS complex differ in some way from the hairpin−DDM and hairpin−SDS complexes of equivalent helicities. However, it is notable that each of these "outlier" mutant hairpins carries an acidic residue introduced to the TM4 sequence (Figure 1), albeit in ES/SE, the Ser to Glu substitution at position 222 in TM4 is paired with a Glu to Ser replacement in the loop region such that global hydropathy is unchanged (Figure 1). The unexpected excluded volumes of these mutants might therefore be traceable to effects on the hairpin−detergent complexes affected by local sequence hydrophobicity near TM4 and/or at the N-terminal end of the loop region.

dx.doi.org/10.1021/bi201853n | *Biochemistry* 2012, 51, 6228−6237

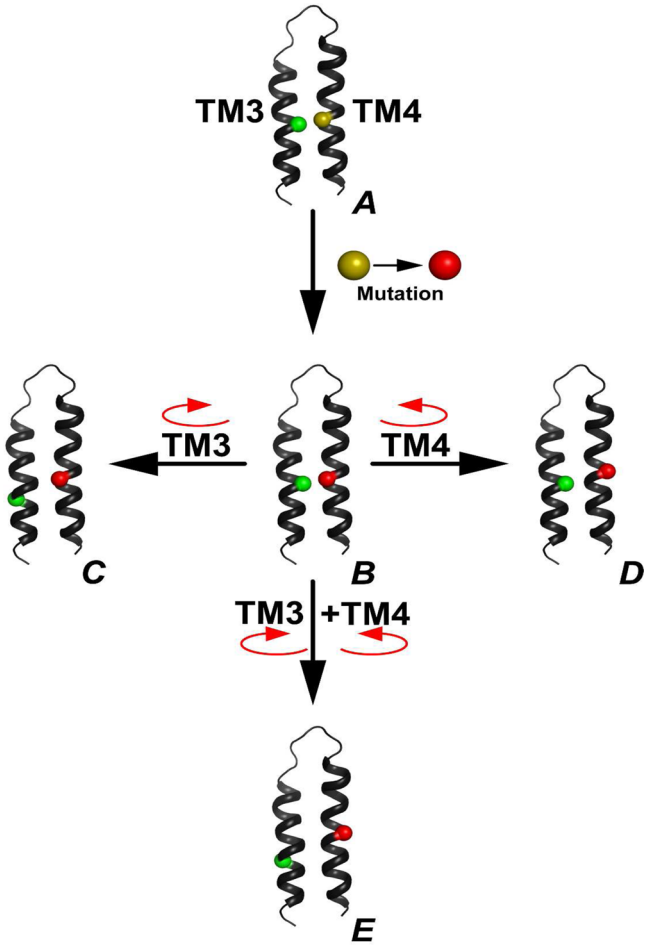

Figure 5. Schematic representation of the structures of detergent-solubilized hairpin constructs. (A) Depiction of a given initial hairpin construct, shown as folded, i.e., in DDM, with reference residues in TM3 (green) and in TM4 (gold) initially in the helix–helix interface. Upon mutation of the TM4 reference residue (rendered as gold to red), the resulting mutant hairpin (B) may remain similarly folded, with the green and red residues persisting in the helix–helix interface. However, the mutation may instead produce a new helix–helix interface, such as (C), where rotation about the TM3 major axis (depicted by a red arrow) now exposes the face containing the green residue to detergent, (D) where rotation about the TM4 major axis exposes the face containing the red residue to detergent, or (E) where rotation about both axes exposes both residues to detergent. Depending upon which structure results from the mutation, the overall helical faces consequently exposed to detergent will produce protein–detergent interactions as a function of the residues in the exposed face(s), largely dependent upon their combined net hydropathy. See text for a further discussion.

Characteristics of Compact Hairpin–Detergent Complexes. While pyrene excimer fluorescence techniques have been used extensively to study folding of soluble proteins [ref 45; see ref 49 for review], its application to membrane proteins has been limited.[32,47,48] However, given the dearth of high-resolution structures available for membrane proteins, we undertook to employ this method as an orthogonal technique to the SEC and CD determinations described herein. We did so with the knowledge that engineering two bulky pyrene moieties into a potentially folded hairpin could themselves impact both folding and local hydrophobicity of our hairpin constructs. In addition, while one might expect the WT sequence to exhibit a well-folded structure in DDM, a homology model of human CFTR that agrees with extensive biochemical data shows TM3/4 with good interhelical contacts in the helical portions close to the short loop region;[50] according to this model, however, the TM3 and TM4 helix ends—at least in the intact CFTR membrane domain—may not be close in space. We were thus excited to observe that solubilization by DDM supports a distance <10 Å between pyrene molecules conjugated at the ends of TM3 and TM4, giving rise to a subset of "compact" mutants (P205S, E217V, E217F, and A204L) (Figure 4B, left). Interestingly, the "compact" subset of mutants exhibits the highest levels of helicity in DDM (compare Figure 4B, left and Figure 2A, left), and these mutants are among the five hairpin–DDM complexes with the largest apparent excluded volumes as assessed by SEC (compare Figure 4B, left and Figure 3B). What appears to be at first a contradictory relationship is actually evidence that hairpin constructs adopt a compact hairpin structure in the mild detergent, where the main variable dictating the larger SEC volumes would be detergent–protein interactions (see Figure 5).

Particularly in SDS, studies of sequence-dependent migration rates on SDS-PAGE indicate that SDS is attracted to hydrophobic residues[31]—including those in loop regions—such that SDS "coating" can readily transform potentially folded hairpins into extended helical rods. Consistent with this possibility, the "high helicity" group of SDS-solubilized mutants (E217F, E217V, and ES/SE) has E:M ratios that do not exceed the negative control. Alternatively, the fact that little excimer fluorescence is observed in SDS may, at least for some mutants, be a consequence of the tendency of this detergent to fray helix ends, as discussed above.

Implications for Detergent Selection. Because changes in helical secondary structure as a function of hydrophobicity are comparable in magnitude in both DDM and SDS, and because we observed that DDM does not promote universally compact conformations among hairpin mutants, our results suggest that no single detergent will be found that does not discriminate to a significant extent on the basis of membrane protein sequence. Thus, levels of secondary structure even in a detergent considered "mild" appear highly sensitive to even a single point mutant (in the present case, one among 87 residues). Changes in protein structure/stability introduced by mutations may thus ultimately be traceable to protein–detergent interactions rather than to specific alteration/disruption of protein–protein contacts per se. Care should accordingly be taken to account for changes in secondary structure and/or alterations in the morphology of the protein–detergent complex when residue substitutions are introduced into membrane proteins, even in "mild" detergents.

AUTHOR INFORMATION

Corresponding Author

*Tel (01) 416 813-5924; Fax (01) 416 813-5005; e-mail deber@sickkids.ca.

Funding

This work was supported, in part, by grants to C.M.D. from the Canadian Institutes of Health Research (CIHR FRN-5810) and the Canadian Cystic Fibrosis Foundation. A.R. received a Research Training Center (RESTRACOMP) postdoctoral award from the Hospital for Sick Children. V.G.N. is the recipient of a Doctoral Training Award from the Fonds de la Recherche en Santé du Quebec (FRSQ) and a Banting and Best Canada Graduate Scholarship from CIHR.

Notes

The authors declare no competing financial interest.

■ ACKNOWLEDGMENTS

We thank Mira Glibowicka for expert technical assistance in expression and purification of hairpin proteins and Dr. David Tulumello for useful discussions.

■ ABBREVIATIONS

CD, circular dichroism; CFTR, cystic fibrosis transmembrane conductance regulator; cmc, critical micelle concentration; DDM, *n*-dodecyl-*β*-D-maltoside; E:M, excimer:monomer ratio; SDS, sodium dodecyl sulfate; SEC, size-exclusion chromatography; TM, transmembrane; WT, wild-type.

■ REFERENCES

(1) Wallin, E., and von Heijne, G. (1998) Genome-wide analysis of integral membrane proteins from eubacterial, archaean, and eukaryotic organisms. *Protein Sci. 7*, 1029−1038.
(2) Otzen, D. (2011) Protein-surfactant interactions: a tale of many states. *Biochim. Biophys. Acta 1814*, 562−591.
(3) Popot, J. L. (2010) Amphipols, nanodiscs, and fluorinated surfactants: three nonconventional approaches to studying membrane proteins in aqueous solutions. *Annu. Rev. Biochem. 79*, 737−775.
(4) le Maire, M., Champeil, P., and Moller, J. V. (2000) Interaction of membrane proteins and lipids with solubilizing detergents. *Biochim. Biophys. Acta 1508*, 86−111.
(5) Prive, G. G. (2007) Detergents for the stabilization and crystallization of membrane proteins. *Methods 41*, 388−397.
(6) Tulumello, D. V., and Deber, C. M. (2012) Efficiency of detergents at maintaining membrane protein structures in their biologically relevant forms. *Biochim. Biophys. Acta, Biomembr. 1818*, 1351−1358.
(7) Imamura, T. (2006) Protein-Surfactant Interactions, in *Encyclopedia of Surface and Colloid Science* (Somasundaran, P., Ed.) 2nd ed., pp 5251−5263, Taylor & Francis, New York.
(8) O'Malley, M. A., Helgeson, M. E., Wagner, N. J., and Robinson, A.S. (2011) Toward Rational Design of Protein Detergent Complexes: Determinants of Mixed Micelles That Are Critical for the In Vitro Stabilization of a G-Protein Coupled Receptor. *Biophys. J. 101*, 1938−1948.
(9) Joh, N. H., Min, A., Faham, S., Whitelegge, J. P., Yang, D., Woods, V. L., and Bowie, J. U. (2008) Modest stabilization by most hydrogen-bonded side-chain interactions in membrane proteins. *Nature 453*, 1266−1270.
(10) Yohannan, S., Yang, D., Faham, S., Boulting, G., Whitelegge, J., and Bowie, J. U. (2004) Proline substitutions are not easily accommodated in a membrane protein. *J. Mol. Biol. 341*, 1−6.
(11) Faham, S., Yang, D., Bare, E., Yohannan, S., Whitelegge, J. P., and Bowie, J. U. (2004) Side-chain contributions to membrane protein structure and stability. *J. Mol. Biol. 335*, 297−305.
(12) Lau, F. W., and Bowie, J. U. (1997) A method for assessing the stability of a membrane protein. *Biochemistry 36*, 5884−5892.
(13) Otzen, D. E. (2003) Folding of DsbB in mixed micelles: a kinetic analysis of the stability of a bacterial membrane protein. *J. Mol. Biol. 330*, 641−649.
(14) Curnow, P., and Booth, P. J. (2009) The transition state for integral membrane protein folding. *Proc. Natl. Acad. Sci. U. S. A. 106*, 773−778.
(15) Curnow, P., and Booth, P. J. (2007) Combined kinetic and thermodynamic analysis of alpha-helical membrane protein unfolding. *Proc. Natl. Acad. Sci. U. S. A. 104*, 18970−18975.
(16) Fisher, L. E., Engelman, D. M., and Sturgis, J. N. (2003) Effect of detergents on the association of the glycophorin a transmembrane helix. *Biophys. J. 85*, 3097−3105.
(17) Ivanov, A. V., Gable, M. E., and Askari, A. (2004) Interaction of SDS with Na+/K+-ATPase: SDS-solubilized enzyme retains partial structure and function. *J. Biol. Chem. 279*, 29832−29840.
(18) Ohnishi, S., and Kameyama, K. (2001) Escherichia coli OmpA retains a folded structure in the presence of sodium dodecyl sulfate due to a high kinetic barrier to unfolding. *Biochim. Biophys. Acta 1515*, 159−166.
(19) Renthal, R. (2006) An unfolding story of helical transmembrane proteins. *Biochemistry 45*, 14559−14566.
(20) Chill, J. H., Louis, J. M., Miller, C., and Bax, A. (2006) NMR study of the tetrameric KcsA potassium channel in detergent micelles. *Protein Sci. 15*, 684−698.
(21) Hirokawa, T., Boon-Chieng, S., and Mitaku, S. (1998) SOSUI: classification and secondary structure prediction system for membrane proteins. *Bioinformatics 14*, 378−379.
(22) Rost, B., Casadio, R., Fariselli, P., and Sander, C. (1995) Transmembrane helices predicted at 95% accuracy. *Protein Sci. 4*, 521−533.
(23) Juretic, D., Zoranic, L., and Zucic, D. (2002) Basic charge clusters and predictions of membrane protein topology. *J. Chem. Inf. Comput. Sci. 42*, 620−632.
(24) Tusnady, G. E., and Simon, I. (2001) The HMMTOP transmembrane topology prediction server. *Bioinformatics 17*, 849−850.
(25) Deber, C. M., Wang, C., Liu, L. P., Prior, A. S., Agrawal, S., Muskat, B. L., and Cuticchia, A. J. (2001) TM Finder: a prediction program for transmembrane protein segments using a combination of hydrophobicity and nonpolar phase helicity scales. *Protein Sci. 10*, 212−219.
(26) Viklund, H., and Elofsson, A. (2008) OCTOPUS: improving topology prediction by two-track ANN-based preference scores and an extended topological grammar. *Bioinformatics 24*, 1662−1668.
(27) Jones, D. T. (2007) Improving the accuracy of transmembrane protein topology prediction using evolutionary information. *Bioinformatics 23*, 538−544.
(28) Cserzo, M., Wallin, E., Simon, I., von Heijne, G., and Elofsson, A. (1997) Prediction of transmembrane alpha-helices in prokaryotic membrane proteins: the dense alignment surface method. *Protein Eng. 10*, 673−676.
(29) Bernsel, A., Viklund, H., Falk, J., Lindahl, E., von Heijne, G., and Elofsson, A. (2008) Prediction of membrane-protein topology from first principles. *Proc. Natl. Acad. Sci. U. S. A. 105*, 7177−7181.
(30) Viklund, H., and Elofsson, A. (2004) Best alpha-helical transmembrane protein topology predictions are achieved using hidden Markov models and evolutionary information. *Protein Sci. 13*, 1908−1917.
(31) Rath, A., Glibowicka, M., Nadeau, V. G., Chen, G., and Deber, C. M. (2009) Detergent binding explains anomalous SDS-PAGE migration of membrane proteins. *Proc. Natl. Acad. Sci. U. S. A. 106*, 1760−1765.
(32) Therien, A. G., and Deber, C. M. (2002) Interhelical packing in detergent micelles. Folding of a cystic fibrosis transmembrane conductance regulator construct. *J. Biol. Chem. 277*, 6067−6072.
(33) Therien, A. G., Glibowicka, M., and Deber, C. M. (2002) Expression and purification of two hydrophobic double-spanning membrane proteins derived from the cystic fibrosis transmembrane conductance regulator. *Protein Expression Purif. 25*, 81−86.
(34) De Grip, W. J., and Bovee-Geurts, P. H. M. (1979) Synthesis and properties of alkylglucosides with mild detergent action: improved synthesis and purification of beta-1-octyl-, -nonyl-, and -decyl-glucose. Synthesis of beta-1-undecylglucose and beta-1-dodecylmaltose. *Chem. Phys. Lipids 23*, 321−335.
(35) Drummond, C. J., Warr, G. G., Grieser, F., Ninham, B. W., and Evans, D. F. (1985) Surface properties and micellar interfacial microenvironment of n-dodecyl *β*-D-maltoside. *J. Phys. Chem. 89*, 2103−2109.
(36) Kjellin, U. R. M., Claesson, P. M., and Vulfson, E. N. (2001) Studies of N-Dodecyllactobionamide, Maltose 6′-O-Dodecanoate, and

Octyl-β-glucoside with Surface Tension, Surface Force, and Wetting Techniques. *Langmuir 17*, 1941−1949.
(37) Sjogren, H., Ericsson, C. A., Evenas, J., and Ulvenlund, S. (2005) Interactions between charged polypeptides and nonionic surfactants. *Biophys. J. 89*, 4219−4233.
(38) Riordan, J. R., Rommens, J. M., Kerem, B., Alon, N., Rozmahel, R., Grzelczak, Z., Zielenski, J., Lok, S., Plavsic, N., Chou, J. L., et al. (1989) Identification of the cystic fibrosis gene: cloning and characterization of complementary DNA. *Science 245*, 1066−1073.
(39) Mulvihill, C. M., and Deber, C. M. (2010) Evidence that the translocon may function as a hydropathy partitioning filter. *Biochim. Biophys. Acta, Biomembr. 1798*, 1995−1998.
(40) Wehbi, H., Gasmi-Seabrook, G., Choi, M. Y., and Deber, C. M. (2008) Positional dependence of non-native polar mutations on folding of CFTR helical hairpins. *Biochim. Biophys. Acta 1778*, 79−87.
(41) Wehbi, H., Rath, A., Glibowicka, M., and Deber, C. M. (2007) Role of the extracellular loop in the folding of a CFTR transmembrane helical hairpin. *Biochemistry 46*, 7099−7106.
(42) Choi, M. Y., Cardarelli, L., Therien, A. G., and Deber, C. M. (2004) Non-native interhelical hydrogen bonds in the cystic fibrosis transmembrane conductance regulator domain modulated by polar mutations. *Biochemistry 43*, 8077−8083.
(43) Kunji, E. R., Harding, M., Butler, P. J., and Akamine, P. (2008) Determination of the molecular mass and dimensions of membrane proteins by size exclusion chromatography. *Methods 46*, 62−72.
(44) le Maire, M., Viel, A., and Moller, J. V. (1989) Size exclusion chromatography and universal calibration of gel columns. *Anal. Biochem. 177*, 50−56.
(45) Sahoo, D., Narayanaswami, V., Kay, C. M., and Ryan, R. O. (2000) Pyrene excimer fluorescence: a spatially sensitive probe to monitor lipid-induced helical rearrangement of apolipophorin III. *Biochemistry 39*, 6594−6601.
(46) Lehrer, S. S. (1997) Intramolecular pyrene excimer fluorescence: a probe of proximity and protein conformational change. *Methods Enzymol. 278*, 286−295.
(47) Jung, K., Jung, H., Wu, J., Prive, G. G., and Kaback, H. R. (1993) Use of site-directed fluorescence labeling to study proximity relationships in the lactose permease of Escherichia coli. *Biochemistry 32*, 12273−12278.
(48) Jung, K., Jung, H., and Kaback, H. R. (1994) Dynamics of Lactose Permease of Escherichia coli Determined by Site-Directed Fluorescence Labeling. *Biochemistry 33*, 3980−3985.
(49) Bains, G., Patel, A. B., and Narayanaswami, V. (2011) Pyrene: A Probe to Study Protein Conformation and Conformational Changes. *Molecules 16*, 7909−7935.
(50) Norimatsu, Y., Ivetac, A., Alexander, C., Kirkham, J., O'Donnell, N., Dawson, D. C., and Sansom, M. S. P. (2012) Cystic Fibrosis Transmembrane Conductance Regulator: A Molecular Model Defines the Architecture of the Anion Conduction Path and Locates a "Bottleneck" in the Pore. *Biochemistry 51*, 2199−2212.